

Personalized Face Privacy Protection From a Single Image

Zachary Yahn, Fatih Ilhan, Tiansheng Huang, Selim Tekin,
Sihao Hu, Yichang Xu, Margaret Loper, Ling Liu, *Fellow, IEEE*

Abstract—Photos of faces uploaded online are vulnerable to malicious actors who can scrape facial images from online sources and intrude on personal privacy via unauthorized use of facial recognition models. This paper presents FACECLOAK, a novel personalized face privacy protection system, which can generate defensive identity-specific universal face privacy masks from a single image of a user, causing facial recognition to fail. FACECLOAK introduces a three-stage personalized face perturbation learning methodology: (1) It generates a small set of high-variety synthetic face images of a person based on a single image of the person. (2) It learns face cloaking by adding more protection to key facial-identity leakage regions through iterative perturbation generation over the small set of synthetic images, effectively shifting a user’s identity embedding towards a distant anchor identity and away from a similar one. (3) It generates a personalized identity-protective mask in the form of pixel-wise cloaking, which is light-weight and can be efficiently applied to any facial image of a user while maintaining good perceptual quality. Extensive experiments on three popular face datasets across ten recognition models show the effectiveness of FACECLOAK compared to 29 other existing representative methods. Code is available here.

Index Terms—Facial recognition, privacy protection, adversarial machine learning

I. INTRODUCTION

Facial Recognition (FR) has long been an important concern for individual privacy. People wish to post their face photos online to socialize, blog, network, and connect with their colleagues, families, and friends, but they do not want unauthorized collection of their identities in large-scale databases. These databases can support infringements on real-world privacy by individuals, such as via stalking and identity fraud [1], [2], as well as by corporations, such as via surveillance, targeted advertisements, and tracking [3]. Examples include PimEyes [4], which provides a searchable database of public facial photos, and Clearview AI [5], which provides facial data to governments. In light of these threats to privacy and given the prevalence of open-source facial recognition models [6]–[9], there is a pressing need to protect user images uploaded online from unwanted facial recognition while maintaining image quality.

A popular defense against unauthorized facial recognition is to subtly perturb a person’s face images with strategic noise (often dubbed a ‘cloak’) to transpose their embeddings to a different latent identity class prior to uploading. However, most existing face perturbation methods require numerous backpropagation calls on a surrogate model [10]–[13] or inference on a large generative model [14]–[17] for every

new image, which may be prohibitively expensive for the average user. Instead of generating a new mask for each image, identity-specific (often dubbed ‘universal’) perturbations optimize a personalized defensive perturbation once for each user [18]. Once generated, such perturbations can be applied to new images of that user trivially. This presents a new set of problems: images provided by users may not be sufficiently representative, the user may not have enough images available to supply the learning process, or the privacy-minded user may not want to share many images of themselves in the first place.

With these problems in mind, we present FACECLOAK, a novel three-stage system which needs only one face image from a user to generate their identity-specific face privacy cloak. First, we generate a small set of diverse, high-quality synthetic images using a single seed image provided by the user. These synthetic images portray the user with varying expressions, lighting, poses, clothing, and backgrounds. Second, we optimize a personalized identity-specific privacy perturbation over the set of synthetic images to shift their embeddings towards a distant latent identity class. We constrain this optimization with a perturbation budget hyperparameter to ensure that the images perturbed with the identity-specific face privacy cloak will maintain high perceptual quality. Third, FACECLOAK provides a personalized identity-specific face perturbation mask that can be applied to any new image of the user through the combination of diverse perturbation focusing methods, e.g., Region-Sticker, Learnable Attention, and High-Pass Mask.

We validate our approach with experiments on three face datasets with ten facial recognition models compared with 29 existing representative identity-specific and image-specific face perturbation methods. Our results show that FACECLOAK substantially outperforms all other identity-specific and image-specific methods in the literature. We also visually compare FACECLOAK to examples from the literature to show that it maintains a high perceptual quality for cloaked face images.

II. RELATED WORK

Image-Specific Perturbations. Image-specific perturbations learn a new perturbation for every image regardless of user identity [10]–[13], [19]. Noise-based image-specific methods mainly differ by how different parts of the loss function are constructed, aiming to design an iterative method for optimizing stealthy perturbations [20]. A different thread of image-specific work proposed applying makeup to faces instead of learning noise-based perturbations [21]. Some use generative adversarial networks [22], such as AMT-GAN [14], while others, like DiffAm, [15] use a fine-tuned diffusion model [23]. Similarly, CLIP2Protect [17] uses zero-shot CLIP [24]

Manuscript received April 30, 2026

This work was funded by the GTRI PhD Fellowship.

The authors are with the Georgia Institute of Technology, Atlanta, Georgia, USA. (email: zachary.yahn@gatech.edu)

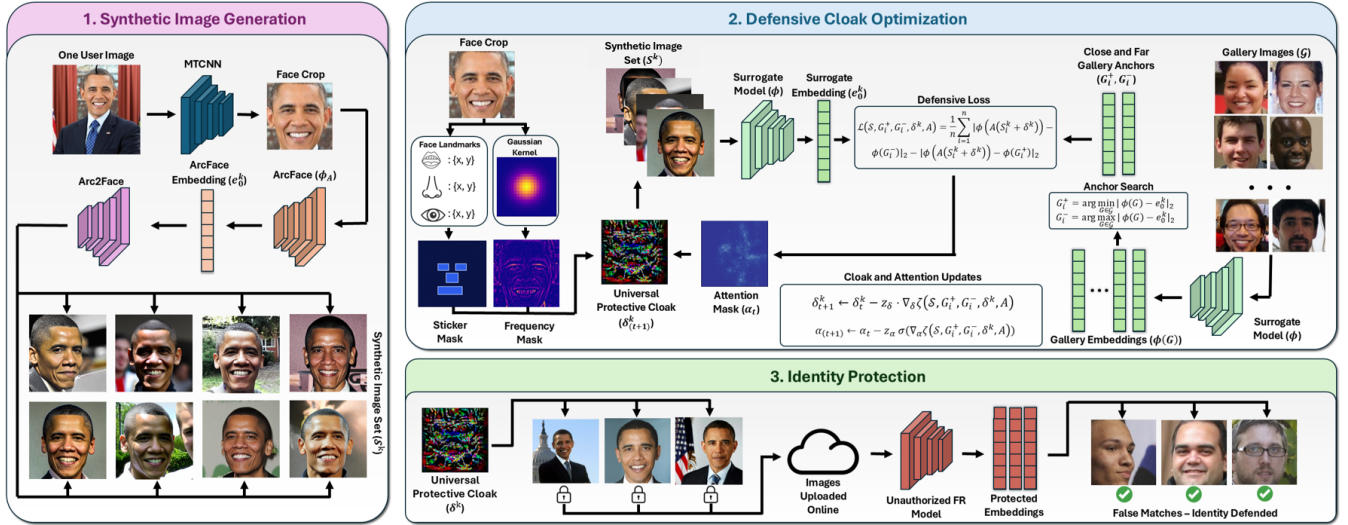


Fig. 1. Overview of FACECLOAK with three progressive stages for face privacy protection: synthetic facial image generation, defensive face cloak optimization, and face-based identity protection. A user only needs to supply a single face image of themselves and will receive an identity-specific face privacy mask that can be rapidly added to any of their face images prior to online release.

embeddings to generate protective makeup. These makeup-based methods achieve high protection rates, but the makeup masks are often highly visible and may be undesirable for people who do not wear makeup.

Existing works have also attempted to combine perturbation-based and makeup-based techniques by training generative models to produce stealthy privacy masks. AdvFaces [25] synthesizes protected face images with a GAN [22]. SD4Privacy [16] uses Stable Diffusion [26] to generate adversarial perturbations that blend with a user’s face. This achieves strong stealthiness scores but lacks the advanced protection of other methods. Adv-CPG [27] proposes a different approach by generating portraits optimized against facial recognition; however, this significantly alters the original image.

Identity-Specific Perturbations. These perturbations are learned offline once and rapidly applied online to any facial images of the user. One Person One Mask (OPOM) [18] produces universal perturbations by optimizing over many images of the same user in order to ensure that the perturbation generalizes to any image of that user. AdvCloak [28] proposes to first learn image-specific perturbations and then combine them into identity-specific perturbations with a GAN [22]. P3-Mask [29] proposes an ensemble method to optimize identity-specific universal perturbations. All of these identity-specific perturbation methods require many images for each user to either train the model, as with AdvCloak, or optimize a perturbation, as with OPOM and P3-Mask. We present FACECLOAK, which only asks each user to provide one face image and learns to generate identity-specific perturbations with high defense performance and high stealthiness.

III. METHODOLOGY

A. Problem Definition and Solution Overview

Given face image $I_0^k \in \mathbb{R}^{H \times W \times C}$ for a person with identity k , the goal of facial privacy protection is to imperceptibly

manipulate the pixels of I_0^k with perturbation $\delta_0^k \in \mathbb{R}^{H \times W \times C}$ so that the embedded representation of I_0^k is closer to an image of a different identity G_n^j than every other image of the person’s actual identity G_n^k in gallery set \mathcal{G} . We formalize this goal as:

$$\|\phi(I_0^k + \delta_0^k) - \phi(G_n^j)\|_2 < \|\phi(I_0^k + \delta_0^k) - \phi(G_n^k)\|_2, \quad (1)$$

$$\forall G^k \in \mathcal{G}, \exists G^j \in \mathcal{G}, j \neq k$$

Here $\phi : \mathbb{R}^{H \times W \times C} \rightarrow \mathbb{R}^d$ is a face image embedding function. Typically, δ_0^k is optimized to protect a single image. In universal facial privacy protection, we attempt to find an identity-specific perturbation δ^k that achieves the above condition when applied to any image of a specific user $I_n^k \in \mathcal{I}^k = \{I_0^k, I_1^k, \dots, I_n^k\}$ where \mathcal{I}^k is the set of publicly available images for a person with identity k .

To find δ^k , we propose a methodology with three phases, as outlined in Figure 1. First, given a single image of a person who wishes to protect their facial privacy, we generate a set of synthetic images of that person. Second, we optimize δ^k over this set of synthetic images, prioritizing key regions or pixels that our method either learns or computes before iterating. Third, we keep this identity-specific δ^k so that when it is added to any image of the person it causes a facial recognition model to misidentify them.

B. Synthetic Image Generation

Previous universal facial privacy protection methods require several user images in order to optimize identity-specific perturbation δ^k [18], [28]–[30]. This is costlier for the user and, given that perturbation optimization is prohibitively expensive for a typical consumer device, it requires them to risk more privacy by transmitting multiple images to the compute server. Instead, we generate synthetic images using just one image from a user. Given user image I_0^k with ArcFace [6]

embedding $e_0^k = \phi_{ArcFace}(I_0^k)$, we generate synthetic images $\mathcal{S}^k = \{S_0^k, S_1^k, \dots, S_n^k\}$ with $S^k = \Psi(e_0^k, n)$, where Ψ is the Arc2Face [31] synthetic image generation model and n is the desired number of synthetic images. In practice, we find that small values of n (e.g. 8) are sufficient to learn strong defensive perturbations due to the quality and variability in synthetic images. Arc2Face naturally generates a wide variety of synthetic user images, including different facial expressions, lighting conditions, pose angles, and clothing.

C. Defensive Cloak Optimization

We optimize δ^k over the set of synthetic user images \mathcal{S}^k to achieve facial privacy protection of any real user image in \mathcal{T}^k . First, we identify near and far anchor images from gallery set \mathcal{G} with respect to the input user image I_0^k with embedding e_0^k :

$$G^+ = \arg \min_{G \in \mathcal{G}} \|\phi(G) - e_0^k\|_2 \quad (2)$$

$$G^- = \arg \max_{G \in \mathcal{G}} \|\phi(G) - e_0^k\|_2 \quad (3)$$

Where G^+ is the nearest image in the gallery set and G^- is the farthest. With these anchors we define our contrastive loss function:

$$\mathcal{L}(\mathcal{S}, G^+, G^-, \delta^k, A) = \frac{1}{n} \sum_{i=1}^n \|\phi(A(S_i^k + \delta^k)) - \phi(G^-)\|_2 - \|\phi(A(S_i^k + \delta^k)) - \phi(G^+)\|_2 \quad (4)$$

In addition to optimizing our perturbation by minimizing this loss, we define three types of focusing functions A that operate on the pixels of the perturbation: Region-Stickers, High-Pass Masks, and Learnable Attention denoted $A_{sticker}$, $A_{highpass}$, and $A_{attention}$, respectively. We define these functions in the following three subsections. We illustrate these and their effects on the generated perturbation in Figure 2. Our optimization methodology applies these in any combination to focus the defensive perturbation on key areas of the facial image and increase protection without sacrificing stealth.

1) *Region-Stickers*: Intuitively, certain areas of a face are more important to facial recognition than others. We propose that these regions include a person’s eyes, nose, and mouth. We hypothesize that larger perturbation magnitudes on these regions may increase protection success by blocking regions that are essential for identification. We extract landmarks $L = \{l_{\text{left eye}}, l_{\text{right eye}}, l_{\text{nose}}, l_{\text{mouth}}\}$ for these with $L = \Lambda(I_0^k)$ where Λ is the MTCNN [32] landmark detection model from InsightFace [33]. We then define bounding boxes around each landmark corresponding to the approximate proportional size of the respective facial feature, which we coin as “stickers:” $B_i = \text{Box}(l_i, w, h) \quad \forall l_i \in L$.

Finally, we combine these stickers into a single region-sticker mask $M_{\text{sticker}} = \bigcup_i B_i$, where every pixel inside the region has a larger perturbation budget than the rest of the mask:

$$\epsilon_{\text{sticker}}(x, y, c) = \begin{cases} \epsilon_A & \text{if } (x, y, c) \in M_{\text{sticker}} \\ \epsilon & \text{otherwise} \end{cases} \quad (5)$$

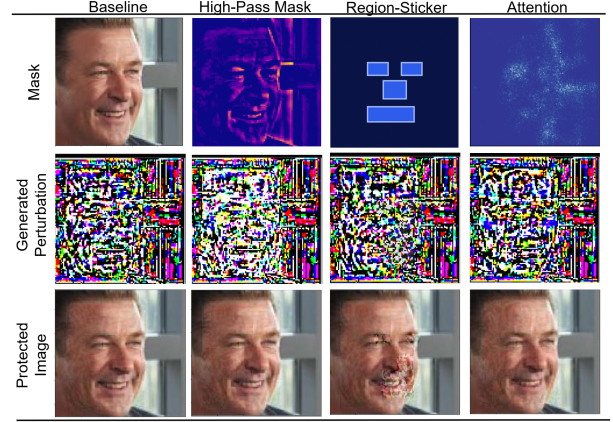


Fig. 2. Visual examples of High-Pass Mask, Region-Sticker, and Learnable Attention mask focusing mechanisms. Each mechanism is designed to emphasize a different aspect of the perturbation with respect to the original image: High-Pass masks hide more noise in high-frequency areas, Region-Sticker masks emphasize perturbations on key identifying features, and Learnable Attention masks add more noise to pixels that are identified as more important to defense during optimization. We use all three in our method.

Region sticker focusing function A_{sticker} thus applies variable perturbation budget $\epsilon_{\text{sticker}}(x, y, c)$ to every pixel with coordinates (x, y) and channel c in a perturbed synthetic image $S_n^k + \delta^k$ during optimization of loss \mathcal{L} in equation 4.

2) *High-Pass Mask*: We observe that noise applied to low-frequency regions of an image, such as a person’s cheek, is much more visible than that applied to high-frequency regions. We hypothesize that hiding larger magnitudes of noise within high-frequency regions will enable stronger protection without sacrificing defense stealthiness. Thus, we propose our second focusing function A_{highpass} . First, we define a high-pass filter $H(I)$ normalized to mean zero and standard deviation one:

$$H(I) = \frac{I - \mathcal{K}_\sigma * I}{\sigma(I - \mathcal{K}_\sigma * I)} \quad (6)$$

Where \mathcal{K}_σ is a Gaussian kernel with standard deviation σ , and $\sigma(\cdot)$ computes standard deviation. Similar to Region-Stickers, we apply A_{highpass} with a piecewise projection perturbation budget according to:

$$\epsilon_{\text{highpass}}(x, y, c) = \begin{cases} \epsilon_A & \text{if } H(I) > \mu \\ \epsilon & \text{otherwise} \end{cases} \quad (7)$$

Where μ is a threshold parameter. The high-pass mask gives only high frequency pixels above the threshold a larger perturbation budget, allowing the optimization to place more noise in those areas.

3) *Learnable Attention*: Both A_{sticker} and A_{highpass} make assumptions about pixel importance prior to perturbation generation. We propose a third focusing function, $A_{\text{attention}}$, that learns which pixels are most important to face privacy protection as perturbation generation iterates. We hypothesize that these important pixels are non-obvious and may not be localized to key facial features or high frequency regions, meaning they should be learned instead.

TABLE I

IDENTITY-SPECIFIC METHODS COMPARISON. PROTECTION SUCCESS RATE (PSR %) OF FACECLOAK DEFENSE UNDER THE BLACK-BOX FACE IDENTIFICATION TASK ON THE PRIVACY-COMMONS DATASET. BOLDDED AND IN BLUE IS BEST, UNDERLINED IS SECOND BEST FOR EACH SURROGATE MODEL AND EACH TARGET MODEL. \uparrow / \downarrow SHOW THE DIFFERENCE IN PERFORMANCE BETWEEN FACECLOAK AND THE NEXT BEST METHOD.

Surrogate Model	Method	ArcFace		CosFace		SFace		MobileNet		SENet		IR50		Average	
		Top-1	Top-5	Top-1	Top-5	Top-1	Top-5	Top-1	Top-5	Top-1	Top-5	Top-1	Top-5	Top-1	Top-5
ArcFace	GD-UAP [34]	6.3	2.7	3.1	1.6	3.0	1.5	8.7	3.5	5.8	2.7	3.0	1.5	5.0	2.3
	GAP [35]	30.7	20.7	19.7	13.9	23.9	15.9	33.6	20.8	31.0	20.1	13.1	7.4	25.3	16.5
	AdvFaces+ [25]	75.1	65.7	69.3	60.7	73.0	64.5	77.0	65.9	74.5	63.4	71.2	60.8	73.4	63.5
	FI-UAP [18]	72.3	62.4	63.5	53.3	70.3	61.8	73.9	61.8	77.4	67.6	52.4	40.7	68.3	58.0
	OPOM-Affine Hull [18]	73.0	63.1	63.3	53.8	71.1	62.0	74.7	63.0	77.8	68.6	52.7	40.8	68.8	58.6
	OPOM-Class Center [18]	76.9	67.8	69.2	60.3	75.0	67.3	78.4	67.9	82.1	73.4	57.1	45.6	73.1	63.7
	OPOM-Convex Hull [18]	78.0	69.4	70.2	61.4	76.1	68.7	79.2	69.1	82.9	74.2	58.7	47.2	74.2	65.0
	AdvCloak [28]	80.1	71.0	74.7	65.7	78.0	69.7	82.0	71.9	78.1	67.4	77.4	67.5	78.4	68.9
	AdvCloak-Affine Hull [28]	79.5	70.6	74.1	65.1	77.5	69.2	81.9	71.7	77.9	67.4	77.2	67.2	78.0	68.5
	AdvCloak-Class Center [28]	81.1	72.3	75.8	67.5	79.0	71.1	83.8	<u>74.7</u>	80.2	70.9	79.0	69.4	79.8	71.0
	AdvCloak-Convex Hull [28]	81.1	<u>72.7</u>	<u>75.9</u>	<u>67.5</u>	79.1	<u>71.3</u>	<u>83.7</u>	<u>74.3</u>	79.8	70.2	79.0	69.4	79.8	70.9
	Ours	90.0 $\uparrow_{8.9}$	86.2 $\uparrow_{13.5}$	77.2 $\uparrow_{1.3}$	70.1 $\uparrow_{2.6}$	80.5 $\uparrow_{1.4}$	71.7 $\uparrow_{0.4}$	82.2 $\uparrow_{1.6}$	76.0 $\uparrow_{1.3}$	85.9 $\uparrow_{3.0}$	77.3 $\uparrow_{3.1}$	96.9 $\uparrow_{17.9}$	94.7 $\uparrow_{25.3}$	85.4 $\uparrow_{5.6}$	79.3 $\uparrow_{8.3}$
	CosFace	GD-UAP [34]	3.7	1.4	1.1	0.4	1.3	0.4	4.0	1.5	3.2	1.0	1.8	0.6	2.5
GAP [35]		42.3	30.6	25.4	16.5	23.7	16.3	29.6	18.0	31.7	21.1	16.8	10.1	28.2	18.8
AdvFaces+ [25]		73.3	63.1	70	61.4	72.1	63.3	72.0	59.3	70.2	58.0	67.0	56.6	70.8	60.3
FI-UAP [18]		75.1	65.8	67.0	57.9	70.7	62.0	48.6	33.4	60.0	46.4	41.5	29.6	60.5	49.2
OPOM-Affine Hull [18]		76.1	67.4	68.8	60.5	72.5	63.9	50.2	35.2	61.4	49.3	43.7	31.8	62.1	51.3
OPOM-Class Center [18]		80.1	71.8	72.6	64.9	76.5	69.1	53.6	38.9	66.2	53.5	47.2	34.9	66.0	55.5
OPOM-Convex Hull [18]		81.4	73.2	73.9	66.0	<u>77.6</u>	<u>70.7</u>	54.8	39.6	67.3	54.7	48.4	36.3	67.2	56.7
AdvCloak [28]		78.4	68.5	74.3	65.4	76.5	68.1	76.6	64.9	73.6	61.4	72.1	61.2	75.3	64.9
AdvCloak-Affine Hull [28]		77.7	68.1	74.0	65.3	76.3	67.7	76.7	64.7	73.5	61.2	72.1	61.4	75.0	64.7
AdvCloak-Class Center [28]		78.7	69.5	75.4	<u>67.4</u>	77.5	69.6	<u>78.6</u>	<u>68.0</u>	<u>76.0</u>	<u>64.8</u>	<u>74.4</u>	<u>64.3</u>	<u>76.8</u>	<u>67.3</u>
AdvCloak-Convex Hull [28]		79.1	69.7	<u>75.7</u>	67.0	77.4	69.6	78.1	66.8	75.2	63.6	73.6	63.0	76.5	66.6
Ours		88.8 $\uparrow_{7.4}$	84.5 $\uparrow_{11.3}$	84.1 $\uparrow_{8.4}$	77.4 $\uparrow_{10.0}$	81.3 $\uparrow_{3.7}$	73.0 $\uparrow_{2.3}$	82.2 $\uparrow_{3.6}$	75.7 $\uparrow_{7.7}$	86.2 $\uparrow_{10.2}$	77.5 $\uparrow_{12.7}$	97.5 $\uparrow_{23.1}$	95.5 $\uparrow_{31.2}$	86.7 $\uparrow_{9.9}$	80.6 $\uparrow_{13.3}$
Softmax		GD-UAP [34]	6.3	2.7	3.1	1.6	3.0	1.5	8.7	3.5	5.8	2.7	0.3	1.5	4.5
	GAP [35]	17.8	11.4	11.1	7.6	12.5	7.6	21.7	12.0	18.8	11.1	7	3.8	14.8	8.9
	AdvFaces+ [25]	75.3	65.5	70.0	61.5	73.4	65.0	80.7	71.3	77	67.2	72.1	61.8	74.7	65.4
	FI-UAP [18]	65.2	53.6	55.7	45.4	63.1	53.3	66.7	53.2	70.5	59.6	44.3	33.0	60.9	49.7
	OPOM-Affine Hull [18]	65.9	54.6	56.1	46.0	63.8	53.4	67.8	54.5	71.7	60.3	44.0	32.8	61.5	50.3
	OPOM-Class Center [18]	69.0	58.7	60.7	51.0	67.0	59.0	71.7	59.5	75.5	65.3	48.8	37.3	65.6	55.2
	OPOM-Convex Hull [18]	70.7	60.2	61.8	52.1	69.4	60.5	72.6	60.7	76.2	66.4	50.2	38.7	66.8	56.4
	AdvCloak [28]	79.0	69.3	73.8	64.6	77.9	69.6	84.0	75.0	79.7	70.5	77.2	66.3	78.6	69.2
	AdvCloak-Affine Hull [28]	79.2	69.8	74.1	64.8	78.0	69.5	83.7	75.1	79.9	70.7	76.8	66.3	78.6	69.4
	AdvCloak-Class Center [28]	81.6	73.0	76.9	<u>68.6</u>	<u>80.5</u>	<u>72.3</u>	87.3	79.3	<u>83.2</u>	<u>75.6</u>	80.4	70.9	81.7	<u>73.5</u>
	AdvCloak-Convex Hull [28]	80.7	71.7	75.3	66.8	79.6	71.2	86.1	78.2	82.7	74.1	79.1	69.3	80.6	71.9
	Ours	90.0 $\uparrow_{8.4}$	86.4 $\uparrow_{14.7}$	80.7 $\uparrow_{3.8}$	73.8 $\uparrow_{5.2}$	90.3 $\uparrow_{9.8}$	85.0 $\uparrow_{12.7}$	82.4 $\uparrow_{4.9}$	76.4 $\uparrow_{12.9}$	88.3 $\uparrow_{5.1}$	81.0 $\uparrow_{5.4}$	97.9 $\uparrow_{17.5}$	96.7 $\uparrow_{25.8}$	88.3 $\uparrow_{6.6}$	83.2 $\uparrow_{9.9}$

We initialize a per-pixel attention map α according to a uniform random distribution. As perturbation generation iterates, we update α according to:

$$\alpha_{(t+1)} \leftarrow \alpha_t - z_\alpha \zeta \left(\frac{\partial \mathcal{L}(\mathcal{S}, G^+, G^-, \delta^k, A)}{\partial \alpha_t} \right) \quad (8)$$

Where z_α is the learning rate for the attention map and $\zeta(\cdot)$ is a normalization function. We show how to combine this learnable attention map with the perturbation in the next section.

4) *Combining Focal Masks*: Our Region-Sticker, High-Pass, and Learnable Attention masks can be applied individually or in combination. Region-Sticker and High-Pass both operate on the perturbation budget ϵ used by projection operator $\Pi(\cdot)$ during loss optimization. If these regions overlap on a pixel, then the perturbation budget for that pixel is ϵ_A . Learnable attention is applied via element-wise multiplication with the perturbation before the projection operation. We apply these three focusing mechanisms to the perturbation and optimize the loss in Equation 4 via iterative optimization similar to PGD [36]. First, we update the perturbation according to:

$$\delta_{(t+1)}^k \leftarrow \delta_t^k - \lambda \cdot \text{sign}(\nabla_{\delta} \mathcal{L}) \quad (9)$$

Where λ is the step size. Then, we calculate the updated perturbed synthetic image:

$$S_{t+1}^k = S_t^k + \Pi(\delta_t^k \odot \alpha_t^k, \epsilon, -\epsilon) \quad (10)$$

Where Π is a projection function onto a perturbation budget. This hyperparameter is either the baseline value ϵ or a larger value ϵ_A according to the Region-Sticker and High-Pass Masks for each pixel with coordinates (x, y) and channel c :

$$\epsilon_{total}(x, y, c) = \epsilon_{sticker}(x, y, c) \cup \epsilon_{highpass}(x, y, c) \quad (11)$$

We then repeat this process iteratively until the number of iterations is reached.

D. Inference-Time Identity Protection

Synthetic image generation and identity-specific perturbation optimization are offline procedures. Once δ^k is computed, it can be easily applied to any user face image I_0^k via simple element-wise addition. A user only needs to submit a single image of themselves to the perturbation generation process once and they will obtain an identity-specific mask that can be applied without ever sending another image and with trivial computation. We conduct experiments to demonstrate that this mask is effective across a variety of facial recognition models, datasets, and face image examples.

IV. EXPERIMENTS

A. Implementation Details

1) *Evaluation Metrics*: We measure the success of FACECLOAK at protecting facial images on the 1:N identification task and on the 1:1 verification task. Both tasks use two datasets: a probe set and a gallery set. During evaluation, we select an image from the probe set. All other images of the same identity are temporarily added to the gallery set. The selected probe set image is then embedded with the face feature extraction model being evaluated and the probe embedding is compared to the embedding of each image in the gallery set. For Top- n identification, the protection is

TABLE II
IDENTITY-SPECIFIC METHODS COMPARISON. PROTECTION SUCCESS RATE (PSR %) OF FACECLOAK DEFENSE UNDER THE BLACK-BOX FACE IDENTIFICATION TASK ON THE PRIVACY-CELEBS DATASET. BOLDDED AND IN BLUE IS BEST, UNDERLINED IS SECOND BEST FOR EACH SURROGATE MODEL AND EACH TARGET MODEL. \uparrow / \downarrow SHOW THE DIFFERENCE IN PERFORMANCE BETWEEN FACECLOAK AND THE NEXT BEST METHOD.

Surrogate Model	Method	ArcFace		CosFace		SFace		MobileNet		SENet		IR50		Average		
		Top-1	Top-5	Top-1	Top-5	Top-1	Top-5	Top-1	Top-5	Top-1	Top-5	Top-1	Top-5	Top-1	Top-5	
ArcFace	GD-UAP [34]	6.5	2.4	3.4	1.2	4.0	1.3	10.0	3.8	6.4	2.5	3.8	1.3	5.7	2.1	
	GAP [35]	40.8	30.9	29.4	21.5	34.8	26.3	45.6	33.6	39.0	28.3	26.0	17.0	35.9	26.3	
	AdvFaces+ [25]	58.4	46.6	51.8	40.6	56.2	45.3	62.3	47.6	58.8	45.0	52.1	38.0	56.6	43.9	
	FI-UAP [18]	61.9	51.2	47.7	37.4	55.3	45.5	50.9	36.2	54.3	41.2	36.2	25.4	51.0	39.5	
	OPOM-Affine Hull [18]	64.9	54.6	50.6	40.8	58.1	48.9	53.3	38.5	57.2	44.4	38.6	27.3	53.8	42.4	
	OPOM-Class Center [18]	66.9	57.5	53.8	44.5	61.7	53.0	55.1	41.1	60.4	58.1	42.0	30.5	56.7	45.8	
	OPOM-Convex Hull [18]	68.5	<u>59.1</u>	55.0	45.9	63.0	54.0	56.4	41.9	61.7	49.4	43.3	31.7	58.0	47.0	
	AdvCloak [28]	67.7	56.9	60.4	50.3	64.6	55.1	71.8	60.0	67.2	55.0	62.4	50.3	65.7	54.6	
	AdvCloak-Affine Hull [28]	66.8	55.9	59.8	49.2	63.6	53.9	70.3	57.8	65.8	53.2	61.1	48.6	64.6	53.1	
	AdvCloak-Class Center [28]	67.6	56.9	61.0	50.9	64.9	55.3	72.3	60.0	67.9	55.8	62.5	50.4	66.0	54.9	
	AdvCloak-Convex Hull [28]	68.5	57.6	61.4	51.0	65.3	55.8	72.3	60.3	67.9	55.8	62.9	50.7	66.4	55.2	
	Ours	82.2 $\uparrow_{13.7}$	76.3 $\uparrow_{17.2}$	72.7 $\uparrow_{11.3}$	65.6 $\uparrow_{14.3}$	78.9 $\uparrow_{13.6}$	73.2 $\uparrow_{17.4}$	86.7 $\uparrow_{14.4}$	83.6 $\uparrow_{23.3}$	79.5 $\uparrow_{11.6}$	72.5 $\uparrow_{16.7}$	85.1 $\uparrow_{22.2}$	80.6 $\uparrow_{29.9}$	80.9 $\uparrow_{14.5}$	75.3 $\uparrow_{20.1}$	
	CosFace	GD-UAP [30]	7.4	3.0	3.7	1.3	4.2	1.4	10.2	4.2	6.3	2.4	3.8	1.3	5.9	2.3
		GAP [35]	42.5	32.6	30.4	21.7	32.1	23.1	39.6	26.6	37.4	26.9	17.2	9.5	33.2	23.4
AdvFaces+ [25]		57.9	44.7	52.1	40.9	55.6	44.1	58.1	43.1	54.8	40.4	49.8	35.3	54.7	41.4	
FI-UAP [18]		62.1	50.8	50.4	40.3	55.9	46.1	46.1	31.4	48.8	36.0	32.5	21.2	49.3	37.6	
OPOM-Affine Hull [18]		65.0	54.3	54.2	43.9	59.7	49.9	49.1	34.2	52.6	39.5	34.8	23.4	52.6	40.9	
OPOM-Class Center [18]		66.0	56.2	56.6	46.5	61.7	52.5	54.5	35.0	54.3	41.4	36.4	25.1	54.1	42.8	
OPOM-Convex Hull [18]		67.4	<u>58.0</u>	57.9	47.9	63.2	54.1	50.8	35.9	56.1	43.2	37.8	26.3	55.5	44.2	
AdvCloak [28]		67.3	56.5	60.8	50.2	64.4	54.1	69.2	56.5	64.1	51.2	58.5	45.2	64.1	52.3	
AdvCloak-Affine Hull [28]		66.7	55.4	60.5	49.9	64.2	53.4	68.3	55.2	63.4	50.4	57.9	44.4	63.5	51.5	
AdvCloak-Class Center [28]		66.5	54.9	61.1	50.3	64.3	54.1	68.2	55.1	64.7	51.7	59.1	45.4	64.0	51.9	
AdvCloak-Convex Hull [28]		67.4	57.6	61.6	51.0	64.6	54.6	69.2	55.9	65.0	51.9	59.1	45.8	64.5	52.6	
Ours		78.8 $\uparrow_{11.4}$	73.1 $\uparrow_{15.1}$	75.5 $\uparrow_{13.9}$	68.8 $\uparrow_{17.8}$	79.1 $\uparrow_{14.5}$	73.2 $\uparrow_{18.7}$	86.8 $\uparrow_{17.6}$	83.6 $\uparrow_{27.1}$	79.6 $\uparrow_{14.6}$	72.7 $\uparrow_{20.8}$	85.6 $\uparrow_{26.5}$	81.1 $\uparrow_{35.3}$	80.9 $\uparrow_{16.4}$	75.4 $\uparrow_{22.8}$	
Softmax		GD-UAP [30]	6.5	2.4	3.4	1.2	3.6	1.3	10.7	3.8	5.7	2.1	3.1	0.9	5.5	2.0
		GAP [35]	30.3	21.0	21.0	13.3	24.1	16.3	43.4	31.2	33.2	23.0	12.8	6.6	27.5	18.6
	AdvFaces+ [25]	60.1	48.2	53.5	42.4	58.1	47.2	68.5	55.7	63.4	50.4	53.8	41.0	59.6	47.5	
	FI-UAP [18]	51.6	40.6	40.4	30.6	47.9	38.1	55.6	42.2	56.1	44.4	33.3	22.8	47.5	36.5	
	OPOM-Affine Hull [18]	53.3	42.7	42.6	32.6	49.7	40.1	58.0	44.5	58.5	46.4	35.1	23.8	49.5	38.4	
	OPOM-Class Center [18]	56.3	45.7	46.3	36.7	53.9	43.7	61.9	49.2	62.1	51.1	37.4	26.1	53.0	42.1	
	OPOM-Convex Hull [18]	58.3	47.8	48.0	38.4	55.6	45.6	62.8	50.3	63.7	52.5	38.9	27.7	54.6	43.7	
	AdvCloak [28]	66.1	54.4	59.7	49.2	63.7	53.5	72.3	60.0	67.4	55.3	60.0	47.2	64.9	53.3	
	AdvCloak-Affine Hull [28]	65.4	54.0	59.4	48.8	63.0	53.0	71.7	59.3	66.6	53.8	59.2	45.9	64.2	52.5	
	AdvCloak-Class Center [28]	68.3	57.6	62.1	51.8	66.1	56.4	75.9	65.0	71.5	60.0	63.0	50.5	67.8	56.9	
	AdvCloak-Convex Hull [28]	67.4	56.2	61.1	50.2	64.7	54.8	74.4	62.8	69.5	57.3	60.9	48.1	66.3	54.0	
	Ours	78.7 $\uparrow_{10.4}$	73.1 $\uparrow_{15.5}$	73.0 $\uparrow_{10.9}$	65.6 $\uparrow_{13.8}$	81.6 $\uparrow_{15.5}$	76.5 $\uparrow_{20.1}$	86.9 $\uparrow_{11.0}$	83.4 $\uparrow_{18.4}$	80.1 $\uparrow_{8.6}$	74.1 $\uparrow_{14.1}$	85.9 $\uparrow_{22.9}$	82.3 $\uparrow_{31.8}$	81.1 $\uparrow_{13.3}$	75.8 $\uparrow_{18.9}$	

successful if there is no image of the same identity as the probe image in the n most similar images in the gallery set. For verification, the protection is successful if the face image identity is successfully changed to a different identity. We calculate Protection Success Rate (PSR) as the total number of images protected this way divided by the number of images in the probe set. We measure both Top-1 PSR and Top-5 PSR.

2) *Datasets*: We evaluate FACECLOAK against other identity-specific methods on two face identification datasets: Privacy-Commons and Privacy-Celebrities [18]. Privacy-Commons is comprised of 500 identities each with 20 images pulled from the MegaFace Challenge 2 dataset [37]. Of these, 5 images per identity form the probe set. Additionally, the Privacy-Commons gallery contains 10,000 other random MegaFace Challenge 2 images with no identity overlap to the probe set as distractors. To form the Privacy-Celebrities dataset we select 500 identities from MS-Celeb-1M [38] and add five distinct images per identity to the probe set. We add 13,233 images from the Labeled Faces in the Wild dataset [39] to the gallery as distractors.

We evaluate FACECLOAK against image-specific methods on face verification with the CelebA-HQ dataset [40]. We randomly select 1,000 identities with one unique image each and group these into 5 groups. These images are added to both the probe and gallery set. Our defense attempts to change each image in each group to a randomly selected identity, per the experimental settings of previous works [14], [15], [17], [27], [41].

3) *Target FR Models*: We test FACECLOAK on ten different facial recognition models: ArcFace [6], CosFace [7], SFace [9], SENet [42], MobileNet [8], and Inception Resnet-50 (IR50) for identity-specific comparisons, [43], and Inception

Resnet-152 (IR152) [43], Inception Resnet SE 50 (IRSE50) [43], Facenet [44] and MobileFace [45] for image-specific comparisons.

4) *System Settings*: For comparison with other identity-specific methods we select a perturbation budget $\epsilon = 8/255$ to allow for fair comparison with peer works [18], [25], [28], [29]. For image-specific comparisons we select a perturbation budget of $\epsilon = 12/255$ to match peer perturbation levels [14], [15], [27]. We set the Region-Sticker and High-Pass Mask perturbation budget $\epsilon_A = 32/255$ for pixels selected by those methods. For each identity we generate a small set of eight synthetic faces. The universal perturbation is generated on each of these images over ten iterations with a step size of $2/255$.

B. Identity-Specific Comparison Results

We compare FACECLOAK with 11 representative identity-specific methods on Privacy-Commons in Table I and Privacy-Celebrities dataset in Table II. ArcFace [6], CosFace [7], and Softmax are used for surrogate models. For each of these, protected images are evaluated against all six recognition models. Results from the 11 methods are cited from their original papers. FACECLOAK outperforms all comparison methods on all models for both datasets with one exception on the Privacy-Commons dataset (Table I): it shows decreased performance against the AdvCloak-ClassCenter [28] method with MobileNet model [8] under ArcFace and Softmax as the surrogate models. FACECLOAK improves average Top-1 PSR by up to 9.9% and average Top-5 PSR by up to 13.3% on Privacy-Common, and it improves average Top-1 PSR by up to 16.4% and average Top-5 PSR by up to 22.8% on Privacy-Celeb. We make three additional observations. (1) FACECLOAK defensive perturbations are highly transferable,

showing strong protection success rates against all comparison facial recognition models regardless of which surrogate model is used. (2) Our method sees the most improvement on IR50 [43], including 35.8% improvement in Top-5 PSR on Privacy-Celebrities and a Top-1 PSR of 97.9% from perturbations generated against Softmax on Privacy-Commons. (3) On average FACECLOAK improves Top-5 PSR more than it improves Top-1 PSR on both datasets. This can be beneficial in realistic scenarios, where an attacker may compare a user’s face to multiple candidate faces instead of just the single most similar one.

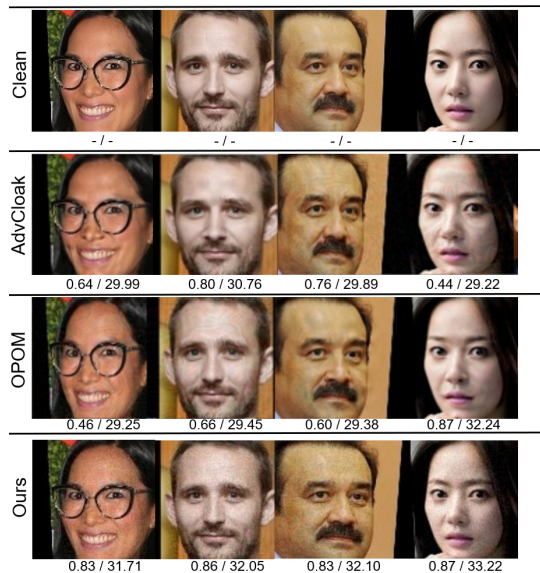


Fig. 3. Visual quality comparison with state of the art identity-specific protection methods. Values shown are SSIM (↑) and PSNR (↑) for that image with respect to the clean version. Images selected by [28].

C. Image-Specific Comparison Results

We compare FACECLOAK with 18 representative image-specific methods on the face verification task on CelebA-HQ [40] in Table III. We adapt our method to be identity-specific by generating a new perturbation for each image. Peer results are from [27]. On IRSE50 [43], Facenet [44], and MobileFace [45], FACECLOAK outperforms all other methods. Interestingly, FACECLOAK is less effective than Adv-CPG [27] on IR152. Overall, our method improves upon the state of the art by 3.6% on average.

V. DISCUSSION

A. Visual Quality Comparison

Perceptual quality is a key challenge for privacy-protecting perturbations. We show that, in addition to providing a strong defense, FACECLOAK has stealthiness comparable to other identity-specific and image-specific methods. In Figure 3 we compare images protected by FACECLOAK with images protected by OPOM [18] and AdvCloak [28]. We also provide SSIM and PSNR perceptual quality metrics beneath each image to measure the perturbation’s stealthiness. We compare

TABLE III
IMAGE-SPECIFIC METHODS COMPARISON. TOP-1 PROTECTION SUCCESS RATE (PSR %) OF FACECLOAK DEFENSE UNDER THE FACE VERIFICATION TASK ON THE CELEBA-HQ DATASET. BOLD IN BLUE IS BEST, UNDERLINED IS SECOND BEST FOR EACH MODEL. ↑ / ↓ SHOW THE DIFFERENCE BETWEEN FACECLOAK AND THE NEXT BEST METHOD.

Method	IR152	IRSE50	Facenet	MobileFace	Average
FGSM [46]	12.1	45.8	1.4	53.0	28.1
MI-FGSM [47]	46.5	70.6	27.1	58.9	50.8
PGD [36]	41.9	63.2	19.6	57.3	45.5
TI-DIM [48]	35.1	62.4	13.7	52.8	41.3
TIP-IM [20]	41.3	57.3	39.1	49.6	46.8
Adv-Hat [49]	5.0	16.9	4.9	12.6	9.9
Adv-Makeup [21]	12.7	20.0	1.4	22.1	14.0
AMT-GAN [14]	12.1	53.3	4.9	48.0	29.5
Clip2Protect [17]	47.6	81.0	42.6	73.6	61.2
GIFT [41]	73.8	83.7	56.5	86.4	75.1
DFPP [50]	46.4	80.6	45.4	72.1	61.1
DiffAM [15]	65.1	89.7	63.0	84.5	75.6
DiffProtect [51]	58.6	79.3	24.7	75.9	59.6
DPG [52]	42.9	62.5	35.8	66.4	51.9
SD4Privacy [16]	66.9	80.0	53.5	74.6	68.7
Adv-Diffusion [53]	52.8	81.7	35.0	70.8	60.1
P3-Mask [29]	73.5	83.4	60.2	69.6	71.7
Adv-CPG [27]	77.0	88.7	<u>63.5</u>	<u>88.0</u>	79.3
Ours	<u>73.5</u> ↓3.5	95.0 ↑5.3	65.5 ↑2.0	97.5 ↑9.5	82.9 ↑3.6

TABLE IV
PERCEPTUAL QUALITY COMPARISON AGAINST SINGLE-IMAGE METHODS ON THE CELEBA-HQ DATASET. BOLD IN BLUE IS BEST. PEER RESULTS FROM [27].

Method	SSIM (↑)	PSNR (↑)	LPIPS (↓)	DISTS (↓)	DreamSim (↓)
Clip2Protect [17]	0.60	19.33	0.30	0.186	0.31
SD4Privacy [16]	0.81	27.01	0.12	0.065	0.22
TIP-IM [20]	0.92	33.19	0.18	0.113	0.36
AdvDiff [53]	0.78	28.31	0.28	0.168	0.13
DiffAM [15]	0.88	20.12	0.14	0.083	0.41
Adv-CPG [27]	0.86	29.88	0.44	0.237	0.48
Ours	0.81	32.63	0.13	0.083	0.21

FACECLOAK’s perturbations to examples from state of the art image-specific methods in Figure 4. Although FACECLOAK adds some noise to the images, it preserves the visual quality of the faces without altering their semantics. Finally, we statistically compare the perceptual quality of images protected by FACECLOAK against seven image-specific methods on 1000 CelebA-HQ images in Table IV. We use classical perceptual quality metrics SSIM and PSNR as well as deep neural network based metrics LPIPS [54], DISTS [55], and DreamSim [56]. We note that FACECLOAK achieves comparable perceptual quality to its peers while offering stronger protection (Table III).

B. Ablation Studies

In Tables V-VII we ablate the values of three key hyperparameters for our method: perturbation budget, number of iterations, and number of synthetic images. As expected, Table V shows that increasing perturbation budget increases protection success rate across all models. For our experiments, we choose perturbation budget values that match those used by peer studies to provide a fair comparison. In Table VI we observe that increasing the number of iterations also increases average protection success rate up until around 10 iterations, after which performance remains roughly the same. For this reason, we select 10 as the number of iterations for our study. Similarly, the results in Table VII show that 8 or more

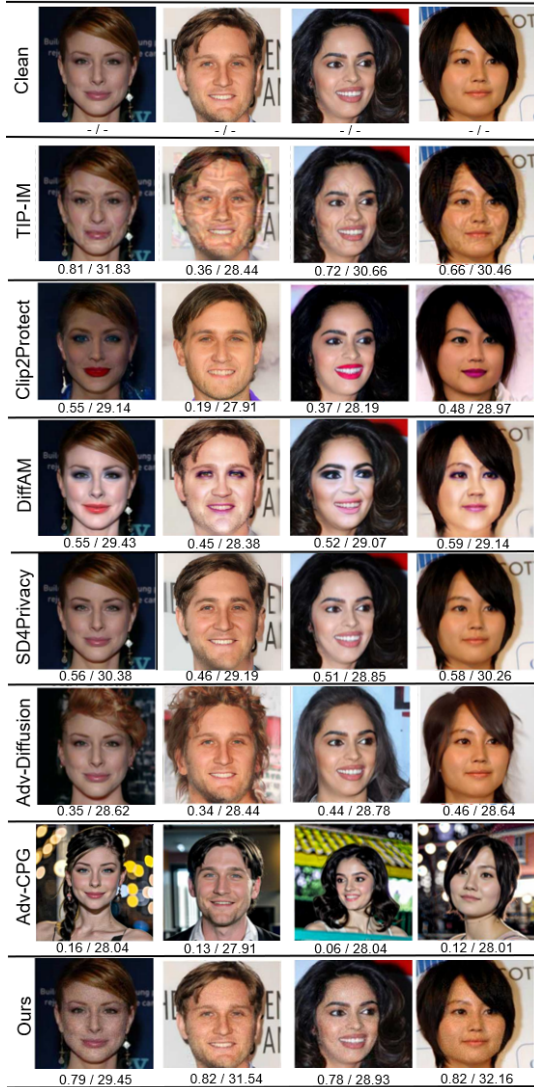


Fig. 4. Visual quality comparison with state of the art image-specific protection methods. Values shown are SSIM (\uparrow) and PSNR (\uparrow) for that image with respect to the clean version. Images selected by [27].

TABLE V
ABLATION STUDY OF PER-MODEL PROTECTION SUCCESS RATE VERSUS PERTURBATION BUDGET VALUE FOR IDENTITY-SPECIFIC METHODS.

Pert. Budget	ArcFace	CosFace	SFace	MobileNet	SENet	IR50	Avg.
2/255	74.8	61.3	60.9	71.8	58.0	75.2	67.0
4/255	77.3	61.7	61.9	71.9	64.0	82.4	69.9
6/255	79.5	64.1	62.2	71.5	69.6	88.4	72.3
8/255	81.1	63.8	64.5	72.0	77.8	90.6	75.0
10/255	81.8	67.5	67.8	71.8	81.8	95.5	77.7
12/255	87.5	70.4	70.5	73.3	88.5	99.3	81.6
14/255	88.4	71.2	71.6	73.4	90.2	97.8	82.1
16/255	94.3	76.6	75.9	73.6	94.4	98.9	85.6

synthetic images have similar protection performance, so we select 8 as the value for our experiments.

We report additional ablation results on the different components of our method in Table VIII, showing the contributions of the individual components of FACECLOAK. Baseline FACECLOAK achieves performance comparable to other universal methods [18], [25], [28]. However, we observe that Region-Stickers (R), Learnable Attention (A), and High-Pass Masks

TABLE VI
ABLATION STUDY OF PER-MODEL PROTECTION SUCCESS RATE VERSUS NUMBER OF ITERATIONS FOR IDENTITY-SPECIFIC METHODS.

Iters.	ArcFace	CosFace	SFace	MobileNet	SENet	IR50	Avg.
2	44.7	27.3	27.8	39.4	35.0	53.2	37.9
4	66.1	47.8	45.1	54.8	57.8	74.1	57.6
6	71.6	54.2	54.5	64.0	66.2	82.0	65.4
8	76.6	57.0	55.8	65.5	69.4	85.2	68.3
10	81.1	63.8	64.4	72.0	77.8	90.6	75.0
12	83.2	68.1	62.3	72.2	77.2	94.3	76.2
14	81.7	64.9	61.4	75.5	78.2	93.3	75.8
16	80.5	63.6	63.6	72.1	74.6	91.8	74.3

TABLE VII
ABLATION STUDY OF PER-MODEL PROTECTION SUCCESS RATE VERSUS NUMBER OF SYNTHETIC IMAGES FOR IDENTITY-SPECIFIC METHODS.

Num. Images	ArcFace	CosFace	SFace	MobileNet	SENet	IR50	Avg.
2	78.4	58.7	58.0	66.2	66.9	84.4	68.8
4	78.7	60.2	59.8	67.4	70.0	90.1	71.0
8	81.1	63.8	64.5	72.0	77.8	90.6	75.0
16	82.7	64.8	65.6	71.6	80.6	94.1	76.6
32	78.5	65.5	66.2	71.6	77.8	93.9	75.6
64	76.7	65.5	66.1	71.7	78.8	96.2	75.8

(H) all contribute to improving the overall performance, with Region-Stickers achieving the largest improvement, followed by Learnable Attention and High-Pass Masks.

Next, we report our study on the differences between real and synthetic images in Figure 5. We record the tradeoff between perceptual quality (SSIM) and protection effectiveness (PSR) averaged across six models on Privacy-Commons for eight real or eight synthetic images. We observe that when FACECLOAK protective perturbations are evaluated on the same model they were trained on (left), real images perform slightly better. When the cloaks are transferred to other models (right), synthetic images achieve identical performance to real ones. This suggests that FACECLOAK’s synthetic perturbation approach can achieve comparable protection to real image approaches without requiring multiple images from the user. We also note that even at very high perceptual quality levels (e.g. SSIM of 0.95) transferred cloaks achieve PSR scores of close to 70%.

C. Robustness to Adversarial Post-Processing

We investigate the performance of FACECLOAK’s perturbations under common post-processing transformations including added noise, Gaussian blur, JPEG compression, brightness shift, and contrast shift in Figure 6. We observe that perturbations optimized against ArcFace as a surrogate and

TABLE VIII
ABLATION STUDY COMPARING DIFFERENT COMPONENTS OF FACECLOAK. TOP-1 AVERAGE AND TOP-5 AVERAGE SHOW THE AVERAGE PROTECTION SUCCESS RATE AGAINST SIX MODELS ON THE INDICATED DATASET. R INDICATES REGION-STICKER, A INDICATES ATTENTION, H INDICATES HIGH-PASS MASK.

Method	Privacy-Common		Privacy-Celebrities	
	Top-1 Avg.	Top-5 Avg.	Top-1 Avg.	Top-5 Avg.
Baseline	76.6	69.2	81.0	75.5
Baseline + R	85.8 \uparrow 9.2	79.5 \uparrow 10.3	86.7 \uparrow 5.7	82.3 \uparrow 6.8
Baseline + R + A	86.6 \uparrow 0.8	80.8 \uparrow 1.3	87.3 \uparrow 0.6	83.1 \uparrow 0.8
FACECLOAK (Baseline + R + A + H)	86.8 \uparrow 0.2	81.0 \uparrow 0.2	87.5 \uparrow 0.2	83.3 \uparrow 0.2

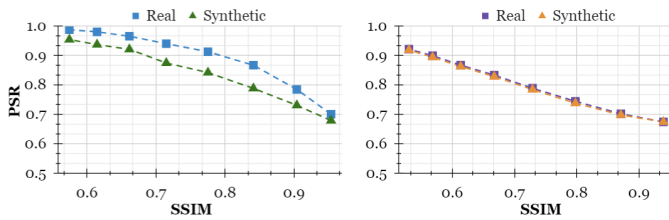


Fig. 5. Perceptual quality and protection success rate tradeoff for eight real or eight synthetic images averaged over six models on Privacy-Commons. Perceptual quality varied by modulating perturbation budget ϵ . Left: perturbations evaluated on same model as training. Right: perturbations transferred from MobileNet to five other models.

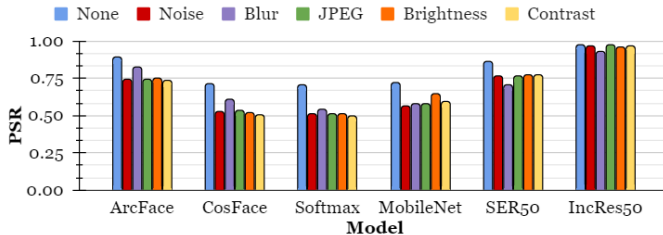


Fig. 6. Robustness of FACECLOAK perturbations under common image transformations. Performance calculated on Privacy-Commons images with an ArcFace surrogate model.

evaluated on other models maintain their robustness under common image transformations. FACECLOAK’s robustness to post-processing varies by transfer model and transformation. For example, perturbations show greater relative resistance to blurring for CosFace than SER50.

VI. CONCLUSION

We present FACECLOAK, a three-stage system for learning facial privacy protection perturbations from a single user image. To our knowledge, ours is the first work to introduce synthetic image generation for identity-specific perturbations, achieving strong per-user protection without requiring multiple user images. Our ablation studies show that our novel face perturbation focusing mechanisms based on key facial landmarks and high frequency face regions increase protection. Experiments also show robustness to common post-processing transformations. Our identity-specific perturbations only need to be generated once for each user, after which they can easily be applied to any image for that user. Extensive experiments show that FACECLOAK improves upon the state of the art in identity-specific and image-specific privacy protection perturbations while maintaining visual quality.

IMPACT STATEMENT

FACECLOAK has the potential to support the digital privacy of individuals who wish to post pictures of themselves online. This is particularly relevant in light of the ever-growing popularity of social media, the widespread scraping of public data for training machine learning systems, and the general commodification of user data. By allowing users to protect all images of themselves with a single image, FACECLOAK lowers the barrier to defending against unwanted facial recognition. While this work is not a catch-all solution to this

complex issue, it is a step towards giving users control over their digital identities.

ACKNOWLEDGEMENT

This research is partially sponsored by the NSF CISE grants 2302720, 2312758, 2038029, an IBM faculty award, and a grant from CISCO Edge AI program. The first author is sponsored by Georgia Tech Research Institute PhD Fellowship Program. FACECLOAK is open sourced at <https://github.com/zacharyyahn/FaceCloak>.

REFERENCES

- [1] AISOnline, “Facial recognition in the united states: Privacy concerns and legal developments,” 2021. [Online]. Available: <https://www.asisonline.org/security-management-magazine/monthly-issues/security-technology/archive/2021/december/facial-recognition-in-the-us>
- [2] Equifax, “Facial recognition and identity risk,” 2023. [Online]. Available: <https://www.equifax.co.uk/resources/identity-protection/facial-recognition-and-identity-risk.html>
- [3] T. N. Y. Times, “The secret company that might end privacy as we know it,” 2021. [Online]. Available: <https://www.nytimes.com/2020/01/18/technology/clearview-privacy-facial-recognition.html>
- [4] PimEyes, “Pimeyes,” 2025. [Online]. Available: <https://pimeyes.com/en>
- [5] C. AI, “Clearview ai,” 2025. [Online]. Available: <https://www.clearview.ai/>
- [6] J. Deng, J. Guo, and S. Zafeiriou, “Arcface: Additive angular margin loss for deep face recognition,” *CoRR*, vol. abs/1801.07698, 2018. [Online]. Available: <http://arxiv.org/abs/1801.07698>
- [7] H. Wang, Y. Wang, Z. Zhou, X. Ji, D. Gong, J. Zhou, Z. Li, and W. Liu, “Cosface: Large margin cosine loss for deep face recognition,” *arXiv preprint arXiv:1801.09414*, 2018.
- [8] A. G. Howard, M. Zhu, B. Chen, D. Kalenichenko, W. Wang, T. Weyand, M. Andreetto, and H. Adam, “Mobilenets: Efficient convolutional neural networks for mobile vision applications,” *arXiv preprint arXiv:1704.04861*, 2017.
- [9] Y. Zhong, W. Deng, J. Hu, D. Zhao, X. Li, and D. Wen, “Sface: Sigmoid-constrained hypersphere loss for robust face recognition,” *IEEE Transactions on Image Processing*, vol. 30, pp. 2587–2598, 2021.
- [10] S. Shan, E. Wenger, J. Zhang, H. Li, H. Zheng, and B. Y. Zhao, “Fawkes: Protecting personal privacy against unauthorized deep learning models,” in *Proc. of USENIX Security*, 2020.
- [11] V. Cherepanova, M. Goldblum, H. Foley, S. Duan, J. Dickerson, G. Taylor, and T. Goldstein, “Lowkey: Leveraging adversarial attacks to protect social media users from facial recognition,” *arXiv preprint arXiv:2101.07922*, 2021.
- [12] E. Wenger, S. Shan, H. Zheng, and B. Y. Zhao, “Sok: Anti-facial recognition technology,” *2023 IEEE Symposium on Security and Privacy (SP)*, pp. 864–881, 2021. [Online]. Available: <https://api.semanticscholar.org/CorpusID:245005742>
- [13] V. Chandrasekaran, C. Gao, B. Tang, K. Fawaz, S. Jha, and S. Banerjee, “Face-off: Adversarial face obfuscation,” *arXiv preprint arXiv:2003.08861*, 2020.
- [14] S. Hu, X. Liu, Y. Zhang, M. Li, L. Y. Zhang, H. Jin, and L. Wu, “Protecting facial privacy: Generating adversarial identity masks via style-robust makeup transfer,” *2022 IEEE/CVF Conference on Computer Vision and Pattern Recognition (CVPR)*, pp. 14994–15003, 2022. [Online]. Available: <https://api.semanticscholar.org/CorpusID:247291928>
- [15] Y. Sun, L. Yu, H. Xie, J. Li, and Y. Zhang, “Diffam: Diffusion-based adversarial makeup transfer for facial privacy protection,” in *Proceedings of the IEEE/CVF Conference on Computer Vision and Pattern Recognition (CVPR)*, June 2024, pp. 24584–24594.
- [16] J. An, W. Zhang, D. Wu, Z. Lin, J. Gu, and W. Wang, “Sd4privacy: Exploiting stable diffusion for protecting facial privacy,” *2024 IEEE International Conference on Multimedia and Expo (ICME)*, pp. 1–6, 2024. [Online]. Available: <https://api.semanticscholar.org/CorpusID:273021715>
- [17] F. Shamshad, M. Naseer, and K. Nandakumar, “Clip2protect: Protecting facial privacy using text-guided makeup via adversarial latent search,” in *Proceedings of the IEEE/CVF Conference on Computer Vision and Pattern Recognition*, 2023, pp. 20595–20605.

- [18] Y. Zhong and W. Deng, "Opom: Customized invisible cloak towards face privacy protection," *IEEE Transactions on Pattern Analysis and Machine Intelligence*, 2022.
- [19] I. Evtimov, P. Sturmfels, and T. Kohno, "FoggySight: A scheme for facial lookup privacy," *arXiv preprint arXiv:2012.08588*, 2020.
- [20] X. Yang, Y. Dong, T. Pang, H. Su, J. Zhu, Y. Chen, and H. W. Xue, "Towards face encryption by generating adversarial identity masks," *2021 IEEE/CVF International Conference on Computer Vision (ICCV)*, pp. 3877–3887, 2020. [Online]. Available: <https://api.semanticscholar.org/CorpusID:237108370>
- [21] B. Yin, W. Wang, T. Yao, J. Guo, Z. Kong, S. Ding, J. Li, and C. Liu, "Adv-makeup: A new imperceptible and transferable attack on face recognition," *arXiv preprint arXiv:2105.03162*, 2021.
- [22] I. Goodfellow, J. Pouget-Abadie, M. Mirza, B. Xu, D. Warde-Farley, S. Ozair, A. Courville, and Y. Bengio, "Generative adversarial networks," *Advances in Neural Information Processing Systems*, vol. 3, 06 2014.
- [23] J. Ho, A. Jain, and P. Abbeel, "Denoising diffusion probabilistic models," *ArXiv*, vol. abs/2006.11239, 2020. [Online]. Available: <https://api.semanticscholar.org/CorpusID:219955663>
- [24] A. Radford, J. W. Kim, C. Hallacy, A. Ramesh, G. Goh, S. Agarwal, G. Sastry, A. Askell, P. Mishkin, J. Clark, G. Krueger, and I. Sutskever, "Learning transferable visual models from natural language supervision," in *International Conference on Machine Learning*, 2021. [Online]. Available: <https://api.semanticscholar.org/CorpusID:231591445>
- [25] D. Deb, J. Zhang, and A. K. Jain, "Advfaces: Adversarial face synthesis," *2020 IEEE International Joint Conference on Biometrics (IJCB)*, pp. 1–10, 2019. [Online]. Available: <https://api.semanticscholar.org/CorpusID:199577709>
- [26] R. Rombach, A. Blattmann, D. Lorenz, P. Esser, and B. Ommer, "High-resolution image synthesis with latent diffusion models," *2022 IEEE/CVF Conference on Computer Vision and Pattern Recognition (CVPR)*, pp. 10674–10685, 2021. [Online]. Available: <https://api.semanticscholar.org/CorpusID:245335280>
- [27] J. Wang, H. Zhang, and Y. Yuan, "Adv-cpg: A customized portrait generation framework with facial adversarial attacks," *2025 IEEE/CVF Conference on Computer Vision and Pattern Recognition (CVPR)*, pp. 21001–21010, 2025. [Online]. Available: <https://api.semanticscholar.org/CorpusID:276929020>
- [28] X. Liu, Y. Zhong, X. Cui, Y. Zhang, P. Li, and W. Deng, "Advcloak: Customized adversarial cloak for privacy protection," *arXiv preprint arXiv:2312.14407*, 2023.
- [29] K.-H. Chow, S. Hu, T. Huang, and L. Liu, "Personalized privacy protection mask against unauthorized facial recognition," in *European Conference on Computer Vision*, 2024.
- [30] Y. Zhang, Z. Yang, T. Wang, Z. Hua, and J. Weng, "Tailor-made face privacy protection via class-wise targeted universal adversarial perturbations," *IEEE Transactions on Dependable and Secure Computing*, vol. 22, no. 5, pp. 5108–5120, 2025.
- [31] F. P. Papantoniou, A. Lattas, S. Moschoglou, J. Deng, B. Kainz, and S. Zafeiriou, "Arc2face: A foundation model for id-consistent human faces," *arXiv preprint arXiv:2403.11641*, 2024.
- [32] K. Zhang, Z. Zhang, Z. Li, and Y. Qiao, "Joint face detection and alignment using multitask cascaded convolutional networks," *IEEE Signal Processing Letters*, vol. 23, no. 10, pp. 1499–1503, 2016.
- [33] J. Deng, J. Guo, X. An, Z. Zhu, and S. Zafeiriou, "Masked face recognition challenge: The insightface track report," *arXiv preprint arXiv:2108.08191*, 2021.
- [34] K. R. Mopuri, A. Ganeshan, and R. V. Babu, "Generalizable data-free objective for crafting universal adversarial perturbations," in *arXiv preprint arXiv: 1801.08092*, 2018.
- [35] O. Poursaeed, I. Katsman, B. Gao, and S. Belongie, "Generative adversarial perturbations," in *Proceedings of the IEEE Conference on Computer Vision and Pattern Recognition*, 2018, pp. 4422–4431.
- [36] A. Madry, A. Makelov, L. Schmidt, D. Tsipras, and A. Vladu, "Towards deep learning models resistant to adversarial attacks," *arXiv preprint arXiv:1706.06083*, 2019.
- [37] A. Nech and I. Kemelmacher-Shlizerman, "Level playing field for million scale face recognition," in *Proceedings of the IEEE Conference on Computer Vision and Pattern Recognition*, 2017.
- [38] Y. Guo, L. Zhang, Y. Hu, X. He, and J. Gao, "Ms-celeb-1m: A dataset and benchmark for large-scale face recognition," *arXiv preprint arXiv:1607.08221*, 2016.
- [39] G. Huang, M. Mattar, T. Berg, and E. Learned-Miller, "Labeled faces in the wild: A database for studying face recognition in unconstrained environments," *Tech. rep.*, 10 2008.
- [40] Z. Liu, P. Luo, X. Wang, and X. Tang, "Deep learning face attributes in the wild," in *Proceedings of International Conference on Computer Vision (ICCV)*, December 2015.
- [41] M. Li, J. Wang, H. Zhang, Z. Zhou, S. shou Hu, and X. Pei, "Transferable adversarial facial images for privacy protection," *Proceedings of the 32nd ACM International Conference on Multimedia*, 2024. [Online]. Available: <https://api.semanticscholar.org/CorpusID:271709384>
- [42] J. Hu, L. Shen, S. Albanie, G. Sun, and E. Wu, "Squeeze-and-excitation networks," *arXiv preprint arXiv:1709.01507*, 2019.
- [43] C. Szegedy, S. Ioffe, V. Vanhoucke, and A. Alemi, "Inception-v4, inception-resnet and the impact of residual connections on learning," *arXiv preprint arXiv:1602.07261*, 2016.
- [44] F. Schroff, D. Kalenichenko, and J. Philbin, "Facenet: A unified embedding for face recognition and clustering," in *Proceedings of the IEEE Conference on Computer Vision and Pattern Recognition*, 2015, pp. 815–823.
- [45] S. Chen, Y. Liu, X. Gao, and Z. Han, "Mobilefacenet: Efficient cnns for accurate real-time face verification on mobile devices," 2018. [Online]. Available: <https://arxiv.org/abs/1804.07573>
- [46] I. J. Goodfellow, J. Shlens, and C. Szegedy, "Explaining and harnessing adversarial examples," *CoRR*, vol. abs/1412.6572, 2014. [Online]. Available: <https://api.semanticscholar.org/CorpusID:6706414>
- [47] Y. Dong, F. Liao, T. Pang, H. Su, J. Zhu, X. Hu, and J. Li, "Boosting adversarial attacks with momentum," *2018 IEEE/CVF Conference on Computer Vision and Pattern Recognition*, pp. 9185–9193, 2017. [Online]. Available: <https://api.semanticscholar.org/CorpusID:4119221>
- [48] Y. Dong, T. Pang, H. Su, and J. Zhu, "Evading defenses to transferable adversarial examples by translation-invariant attacks," *2019 IEEE/CVF Conference on Computer Vision and Pattern Recognition (CVPR)*, pp. 4307–4316, 2019. [Online]. Available: <https://api.semanticscholar.org/CorpusID:102350868>
- [49] S. A. Komkov and A. Petiushko, "Advhat: Real-world adversarial attack on arcface face id system," *2020 25th International Conference on Pattern Recognition (ICPR)*, pp. 819–826, 2019. [Online]. Available: <https://api.semanticscholar.org/CorpusID:201645162>
- [50] F. Shamshad, M. Naseer, and K. Nandakumar, "Makeup-guided facial privacy protection via untrained neural network priors," in *ECCV Workshops*, 2025, pp. 227–246.
- [51] J. Liu, C. P. Lau, and R. Chellappa, "Diffprotect: Generate adversarial examples with diffusion models for facial privacy protection," *ArXiv*, vol. abs/2305.13625, 2023. [Online]. Available: <https://api.semanticscholar.org/CorpusID:258841845>
- [52] Y. Zhang, D. Ye, C. Xie, S. Shen, Z. Liu, J. Deng, and L. Tang, "Dip-watermark: A double identity protection method based on robust adversarial watermark," 2024. [Online]. Available: <https://arxiv.org/abs/2404.14693>
- [53] D. Liu, X. Wang, C. Peng, N. Wang, R. Hu, and X. Gao, "Adv-diffusion: imperceptible adversarial face identity attack via latent diffusion model," in *Proceedings of the AAAI Conference on Artificial Intelligence*, vol. 38, no. 4, 2024, pp. 3585–3593.
- [54] R. Zhang, P. Isola, A. A. Efros, E. Shechtman, and O. Wang, "The unreasonable effectiveness of deep features as a perceptual metric," in *Proceedings of the IEEE conference on computer vision and pattern recognition*, 2018, pp. 586–595.
- [55] K. Ding, K. Ma, S. Wang, and E. P. Simoncelli, "Image quality assessment: Unifying structure and texture similarity," *IEEE transactions on pattern analysis and machine intelligence*, vol. 44, no. 5, pp. 2567–2581, 2020.
- [56] S. Fu, N. Tamir, S. Sundaram, L. Chai, R. Zhang, T. Dekel, and P. Isola, "Dreamsim: Learning new dimensions of human visual similarity using synthetic data," *arXiv preprint arXiv:2306.09344*, 2023.

VII. BIOGRAPHY SECTION

Zachary Yahn graduated from University of Virginia with a BS in Computer Science and in Computer Engineering and from Univerity College Dublin with a MS in Computer Science. He joined the CS PhD program at Georgia Tech in Fall 2024. His work spans adversarial machine learning, privacy, and agentic security, and he has published at top venues including CVPR, ICCV, and IEEE journals.

Fatih Ilhan graduated from Bilkent University, Turkey, with BS and MSc in Computer Science (CS), and joined the CS PhD program in the Georgia Institute of Technology since 2021. Fatih’s research interest lies in efficient AI and Machine Learning systems and algorithms, and published in IEEE and ACM journals, and top conferences, e.g., CVPR, ICDCS, NeurIPS, WWW.

Tiansheng Huang graduated from Southern University, China, with BS and MS and started his CS PhD program in the Georgia Institute of Technology since 2022. He is working on safety alignment algorithms against harmful fine-tuning at user-level and published in IEEE and ACM journals, and top conferences, e.g., CVPR, ICML, ICLR, NeurIPS.

Selim Tekin graduated from Bilkent University, Turkey, with BS and MSc in CS, and joined the CS PhD program in the Georgia Institute of Technology since 2022. Selim’s PhD research interest lies in dynamic routing and ensemble learning for robust and high performance AI and ML systems, and has published in IEEE and ACM journals and top conferences, including ICML, EMNLP, CVPR, NeurIPS, WWW.

Sihao Hu graduated with BS from Zhejiang University, China, MSc in Singapore National University, and joined the CS PhD program in the Georgia Institute of Technology since 2022. Sihao is working on Game AI agents and detection of Fraudulent activities in Decentralized Financial and Crypto Systems, and has published in IEEE and ACM journals, and top conferences like WWW, CVPR, NeurIPS.

Yichang Xu graduated with BS from China Science and Technology University (Talented Class) in 2024 and joined the CS PhD program in the Georgia Institute of Technology since 2024. His research is centered on multi-modal agentic AI systems and algorithms. He has published in ACM journal and top conferences like CVPR and WWW.

Margaret L. Loper is the Associate Director for Operations of the Information & Communications Laboratory (ICL) at the Georgia Tech Research Institute. Her research focus is modeling and simulation, specifically focused on parallel and distributed systems. She previously served as ICL’s Chief Scientist, where she led initiatives on Internet of Things, Information Security and Privacy and Smart Cities. Margaret holds a Ph.D. in CS from the Georgia Institute of Technology.

Ling Liu is a Professor in the School of Computer Science at Georgia Institute of Technology. She directs the research programs in the Distributed Data Intensive Systems Lab (DiSL), examining various aspects of Internet-scale big data powered artificial intelligence (AI) systems, algorithms and analytics, including performance, reliability, privacy, security

and trust. Ling’s current research is supported by National Science Foundation CISE programs, CISCO, and IBM.